

Colored-noise-induced multistability in nonequilibrium phase transitions

Seunghwan Kim,* Seon Hee Park, and C. S. Ryu

*Telecommunication Basic Research Laboratory, Electronics and Telecommunications Research Institute,
P.O. Box 106, Yusong-gu, Taejon 305-600, Korea*

(Received 11 September 1997; revised manuscript received 27 August 1998)

We investigate the colored-noise effect on nonequilibrium phase transitions. A simple model is studied analytically in the presence of a dichotomous multiplicative noise. In the white-noise limit, the model shows a nonequilibrium phase transition. With a finite correlation time of the noise, the system exhibits multistability of ordered and disordered states and as the coupling strength increases, it also shows a reentrant transition into the disordered phase. Numerical simulation results are presented confirming the existence of the multistability and the reentrant transition. [S1063-651X(98)09512-9]

PACS number(s): 05.40.+j, 05.70.Ln, 02.50.Ey, 64.60.Cn

A noise-induced nonequilibrium phase transition in a dynamical system with multiplicative noise has been the topic of much recent investigation [1–10]. While an additive noise in equilibrium provides a disordering effect, restoring a broken symmetry, the multiplicative noise coupled to the state of the system induces an ordered symmetry-breaking state. The interplay of the additive and multiplicative noises produces a reentrant transition, showing the ordered symmetry-breaking state only for intermediate intensities of the multiplicative noise [4,10]. The fluctuating interaction has also been studied, showing the symmetry-breaking transition [7] and noise-enhanced multistability [9]. Multistability shown in a time-delayed system has also been interpreted as a mechanism of perception of ambiguous or reversible figures [11]. Most studies of the noise-induced phase transition have usually considered the multiplicative noise as white. Since the multiplicative noise comes in general from the coupling with an external source, the consideration of the temporal correlation of the noise is realistic.

In this Brief Report we investigate the colored noise effect on the nonequilibrium phase transition. We consider a simple model that shows the nonequilibrium phase transition in the presence of white multiplicative noise. In the model a reentrant transition is also shown, leading to an ordered state only for intermediate intensities of the white multiplicative noise. To study the colored-noise effect we introduce a dichotomous multiplicative noise into the system instead of the white multiplicative noise. For the globally coupled system we obtain the self-consistent equation of the order parameter analytically, assuming that there is no spatial correlation. With the finite correlation time of the dichotomous noise, we show that the system exhibits multistability of the ordered and disordered states and a reentrant transition into the disordered state as the coupling strength increases. A numerical simulation is performed confirming the analytical results.

As in Ref. [4], we consider a dynamical system whose state at time t is described by the set of stochastic variables $\{x_i(t) | i = 1, \dots, N\}$. The time evolution of the system is governed by the stochastic differential equation

$$\frac{dx_i}{dt} = f(x_i) + g(x_i)\eta_i + \frac{D}{z_i} \sum_{j \in n(i)} (x_j - x_i), \quad (1)$$

where D is a coupling constant, $n(i)$ stands for the set of z_i sites coupled with x_i , and η_i is the multiplicative noise. The sum in Eq. (1) describes diffusive coupling, which depends on the difference of two x_i 's. The specific case considered here and analyzed in Ref. [4] is

$$f(x) = -x(1+x^2)^2, \quad g(x) = 1+x^2,$$

which could be the simplest example exhibiting the nonequilibrium phase transition. In this case Eq. (1) is invariant under a symmetric operation

$$x_i \rightarrow -x_i, \quad \eta_i \rightarrow -\eta_i \quad \text{for all } i.$$

This symmetry is broken by the multiplicative noise.

To study the colored noise effect on the system, we consider η_i as the Markovian dichotomous noise that consists of two levels $\{\Delta_-, \Delta_+\}$. This dichotomous noise is characterized by the transition rates $\alpha(\Delta_- \rightarrow \Delta_+)$ and $\alpha(\Delta_+ \rightarrow \Delta_-)$ between two levels. Here we consider the case of symmetric dichotomous noise given by

$$\Delta_+ = -\Delta_- \equiv \Delta, \quad \alpha(\Delta_- \rightarrow \Delta_+) = \alpha(\Delta_+ \rightarrow \Delta_-) \equiv \alpha.$$

Then the noises η_i have zero mean and the correlations

$$\langle \eta_i(t) \eta_j(t') \rangle = \delta_{ij} \frac{\sigma^2}{2\tau} \exp\left[-\frac{|t-t'|}{\tau}\right],$$

where $\sigma \equiv \Delta/\sqrt{\alpha}$ measures the intensity of the dichotomous noise and $\tau \equiv 1/2\alpha$ is the correlation time of the noise. In the limit $\tau \rightarrow 0$, the dichotomous noise $\eta_i(t)$ tends to the white noise $\xi_i(t)$ with correlations $\langle \xi_i(t) \xi_j(t') \rangle = \sigma^2 \delta_{ij} \delta(t-t')$, which is the case studied in Ref. [4].

The composite system, comprising both the state variables $\{x_i\}$ and the dichotomous noises $\{\eta_i\}$, is described analytically by the joint probability distribution $\rho(\{x_i\}, \{\eta_i\}, t)$. This joint probability distribution satisfies the coupled Fokker-Planck equations [12]

*Electronic address: skim@etri.re.kr

$$\begin{aligned} \frac{\partial \rho(\{x_i\}, \{\eta_i\}, t)}{\partial t} = & - \sum_{j=1}^N \frac{\partial}{\partial x_j} \left[f(x_j) + g(x_j) \eta_j \right. \\ & \left. + \frac{D}{z_j} \sum_{k \in n(j)} (x_k - x_j) \right] \rho(\{x_i\}, \{\eta_i\}, t) \\ & - \alpha \sum_{j=1}^N [\rho(\{x_i\}, \{\eta_i\}, t) - \rho_j(\{x_i\}, \{\eta_i\}, t)] \end{aligned} \quad (2)$$

for all configurations of $\{\eta_i\}$. In Eq. (2), $\rho_j(\{x_i\}, \{\eta_i\}, t)$ represents the joint probability distribution $\rho(\{x_i\}, \{\eta_i'\}, t)$ with $\eta_i' = -\delta_{ij}\eta_j + (1 - \delta_{ij})\eta_i$ for all i . In the globally coupled system, since the variables $\{x_i\}$ are statistically independent [7], we assume that there is no spatial correlation in $\rho(\{x_i\}, \{\eta_i\}, t)$ leading to

$$\rho(\{x_i\}, \{\eta_i\}, t) = \prod_{i=1}^N \rho_1(x_i, \eta_i, t),$$

with the normalization condition

$$\sum_{\eta \in \{\Delta, -\Delta\}} \int \rho_1(x, \eta, t) dx = 1.$$

This assumption is confirmed by extensive numerical simulations. For a given i , by the integrations over x_j 's and summations over η_j 's for all $j \neq i$, Eq. (2) reduces to the Fokker-Planck equation for $\rho_1(x, \eta, t)$,

$$\begin{aligned} \frac{\partial \rho_1(x, \eta, t)}{\partial t} = & - \frac{\partial}{\partial x} \{ [f(x) + g(x)\eta + D(m-x)] \rho_1(x, \eta, t) \} \\ & - \alpha [\rho_1(x, \eta, t) - \rho_1(x, -\eta, t)], \end{aligned}$$

where m is the order parameter given by

$$m = \sum_{\eta \in \{\Delta, -\Delta\}} \int x \rho_1(x, \eta, t) dx. \quad (3)$$

The ordered symmetry-breaking state is characterized by the nonzero order parameter m .

The quantity that we are interested in is the probability distribution for the state variable x alone, i.e., $P(x, t) \equiv \rho_1(x, \Delta, t) + \rho_1(x, -\Delta, t)$. Defining $q(x, t) \equiv \rho_1(x, \Delta, t) - \rho_1(x, -\Delta, t)$, we obtain the evolutionary equations for $P(x, t)$ and $q(x, t)$ as

$$\begin{aligned} \frac{\partial P(x, t)}{\partial t} = & - \frac{\partial}{\partial x} \{ [f(x) + D(m-x)] P(x, t) \} \\ & + \Delta g(x) q(x, t), \\ \frac{\partial q(x, t)}{\partial t} = & - \frac{\partial}{\partial x} \{ [f(x) + D(m-x)] q(x, t) \} \\ & + \Delta g(x) P(x, t) - 2\alpha q(x, t). \end{aligned} \quad (4)$$

In the stationary state, we solve Eq. (4) with the boundary condition that there is no probability current at boundary, leading to the stationary probability distribution

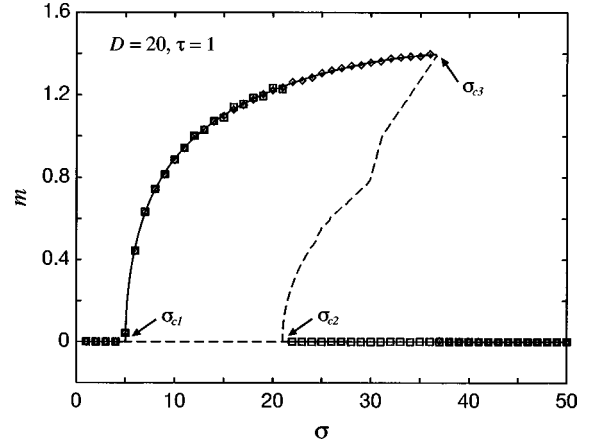


FIG. 1. Plot of the order parameter m as a function of σ at $D = 20$ and $\tau = 1$. Solid and dashed lines are stable and unstable solutions of the self-consistent equation (6), respectively. \diamond and \square represent the order parameter m obtained from the numerical simulations as σ increases from zero and decreases from 50, respectively. σ_{c1} , σ_{c2} , and σ_{c3} are transition points of the triple transitions, disordered state \rightarrow ordered state \rightarrow multistable state \rightarrow disorder state, respectively.

$$\begin{aligned} P(x) = & N_0 \left| \frac{1}{F_+(x)} - \frac{1}{F_-(x)} \right| \\ & \times \exp \left[-\alpha \int^x \left(\frac{1}{F_+(x')} + \frac{1}{F_-(x')} \right) dx' \right], \end{aligned} \quad (5)$$

with

$$F_{\pm}(x) = f(x) \pm \Delta g(x) + D(m-x).$$

In Eq. (5), N_0 is determined by the normalization condition $\int P(x) dx = 1$. $P(x)$ in Eq. (5) has two singular points x_{\pm} , which are roots of $F_{\pm}(x)$, respectively. Since the singular points x_{\pm} are stable fixed points of the deterministic equations $dx/dt = F_{\pm}(x)$, respectively, $P(x)$ is normalizable restricting x in (x_-, x_+) [12]. Equation (3) with Eq. (5) presents the self-consistent equation of the order parameter m as

$$m = G(m) \equiv \int x P(x) dx. \quad (6)$$

In Fig. 1 we show the order parameter m obtained from the self-consistent equation (6) as a function of σ at $D = 20$ and $\tau = 1$. For small $\sigma < \sigma_{c1} \equiv 5.0$, $m = 0$, implying that the system is in a disordered symmetric state. At $\sigma = \sigma_{c1}$, $m = 0$ becomes an unstable solution and a stable solution appears, implying that the system is in an ordered symmetry-breaking state. As σ increases above σ_{c1} , the stable solution increases continuously, leading to the second-order phase transition at $\sigma = \sigma_{c1}$. At $\sigma = \sigma_{c2} \equiv 21.0$, $m = 0$ becomes a stable solution again and an unstable solution appears, leading to a subcritical bifurcation. As σ increases above σ_{c2} , the unstable solution increases. In this case, there are two stable solutions: One is zero and the other is nonzero. This means that the system shows multistability of ordered and disordered states. At $\sigma = \sigma_{c3} \equiv 36.7$, the stable solution with nonzero m and the unstable solution are annihilated, leading to an inverse subcritical bifurcation. Thus, for $\sigma > \sigma_{c3}$, m

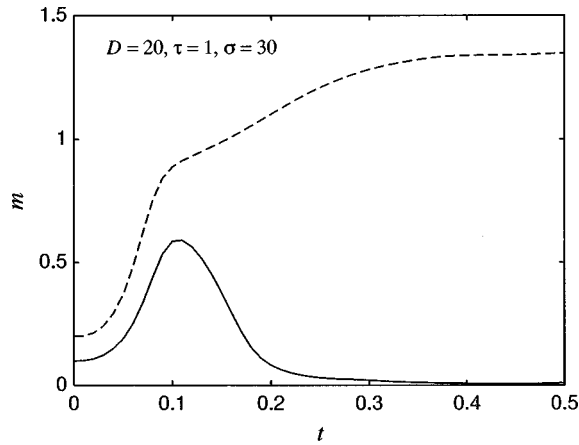


FIG. 2. Plot of time evolutions of the order parameter m obtained by the numerical simulation with different initial configurations for the system of size $N=10^4$ at $D=20$, $\tau=1$, and $\sigma=30$.

$=0$ is only a stable solution, implying that the system is in the disordered symmetric state again.

To confirm the analytical result we have performed a numerical simulation with the stochastic equation (1) for the system of size $N=10^4$. In the simulation we have used the Euler method with discrete time steps of $\Delta t=10^{-4}$. At each run, the first 10^6 time steps have been discarded to achieve a steady state and 5×10^6 time steps have been used to calculate the order parameter m . Figure 1 shows m obtained by the numerical simulation as σ increases and decreases. The numerical data coincide with the analytical stable solution very well. Figure 2 shows the time evolutions of m obtained by the numerical simulation with different initial configurations for the system at $D=20$, $\tau=1$, and $\sigma=30$. While one goes to zero, the other approaches a finite value. This implies that the system is in the multistable phase of the ordered and disordered states.

Figure 3 shows a phase diagram in the σ - τ plane at $D=20$. At $\tau=0$ there is no multistable phase. The ordered phase exists only in the intermediate intensities of σ showing the reentrant transition into the disordered phase as σ increases. As τ increases the multistable phase appears and

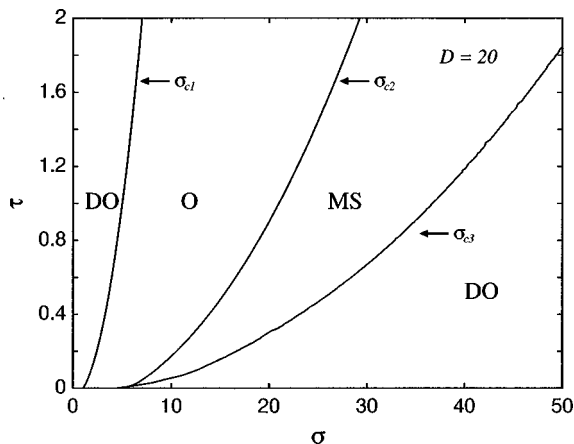


FIG. 3. Plot of phase diagram in the σ - τ plane at $D=20$. DO, O, and MS represent disordered, ordered, and multistable phases, respectively. σ_{c1} , σ_{c2} , and σ_{c3} are transition lines of the triple transitions, DO \rightarrow O \rightarrow MS \rightarrow DO, respectively.

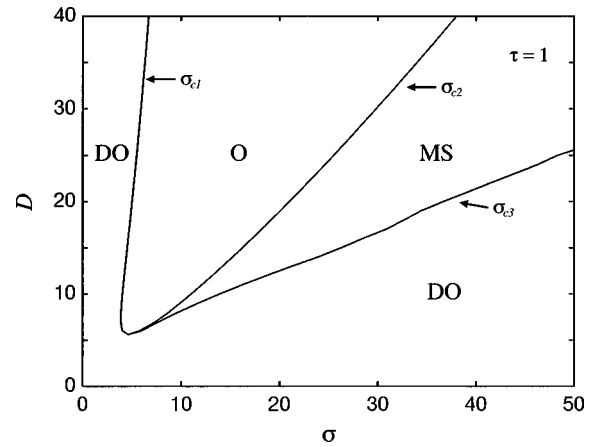


FIG. 4. Plot of the phase diagram in the σ - D plane at $\tau=1$. DO, O, and MS represent disordered, ordered, and multistable phases, respectively. σ_{c1} , σ_{c2} , and σ_{c3} are transition lines of the triple transitions, DO \rightarrow O \rightarrow MS \rightarrow DO, respectively.

expands. The ordered phase also expands. Figure 3 also shows a reentrant transition exhibiting a disordered state for large values of σ . The critical points σ_{c1} , σ_{c2} , and σ_{c3} , at which the triple transitions, disordered phase \rightarrow ordered phase \rightarrow multistable phase \rightarrow disordered phase, occur, respectively, increase monotonically as τ increases. This produces the reentrant transition into the disordered phase as τ increases at a fixed value of $\sigma > \sigma_{c3}$ ($\tau=0$).

Figure 4 shows a phase diagram in the σ - D plane at $\tau=1$. For small $D < D_c \approx 5.6$, the system is in the disordered state regardless of the values of σ . At $D=D_c$, the ordered phase and the multistable phase appear at an intermediate value of σ , $\sigma_0 \approx 4.7$. As D increases the ordered and multistable phases expand. The critical points σ_{c1} , σ_{c2} , and σ_{c3} at which the triple transitions, disordered phase \rightarrow ordered phase \rightarrow multistable phase \rightarrow disordered phase, occur, respectively, increase monotonically as D increases. This produces the reentrant transition into the disordered phase as D increases at a fixed value of $\sigma > \sigma_0$.

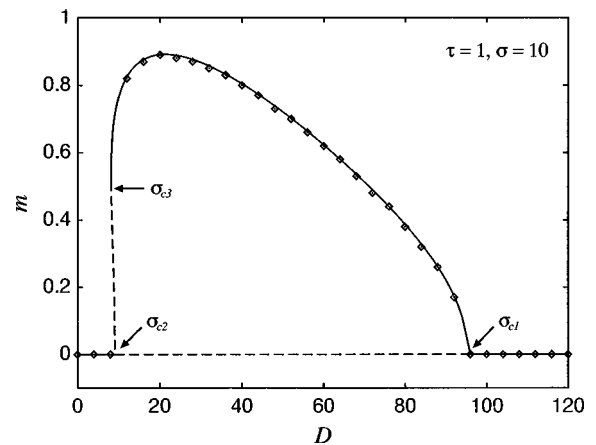


FIG. 5. Plot of the order parameter m as a function of D at $\tau=1$ and $\sigma=10$. Solid and dashed lines are stable and unstable solutions of the self-consistent equation (6), respectively. \diamond represents the order parameter m obtained from the numerical simulation for the system of size $N=10^4$. σ_{c3} , σ_{c2} , and σ_{c1} are transition points of the triple transitions, disordered state \rightarrow multistable state \rightarrow ordered state \rightarrow disordered state, respectively.

Figure 5 shows the order parameter m as a function of D at $\tau=1$ and $\sigma=10$. There are three transition points, $\sigma_{c3}=8.17$, $\sigma_{c2}=9.10$, and $\sigma_{c1}=95.0$, at which the triple transitions, disordered phase \rightarrow multistable phase \rightarrow ordered phase \rightarrow disordered phase, occur, respectively. In Fig. 5 one can see that the large strength of coupling induces disorder in the system. Since the coupling-induced disorder does not exist in the system with white noise, it is a pure colored-noise effect. Numerical simulation confirms the analytical result.

In conclusion, we investigated the colored-noise effect on the nonequilibrium phase transition, considering a simple model under a dichotomous multiplicative noise. We obtained a self-consistent equation of the order parameter analytically. In the white-noise limit, the system shows a non-equilibrium phase transition presenting the ordered phase in the intermediate intensities of the noise. In the presence of a

finite correlation time of the noise, the system has the multistable phase of the ordered and disordered states in addition to the ordered and disordered phases. The transition points of the triple transitions, disordered phase \rightarrow ordered phase \rightarrow multistable phase \rightarrow disordered phase, increase as the correlation time and the coupling strength increase. This produces the reentrant transitions into the disordered phase as the correlation time and the coupling strength increase. The color-induced disorder and coupling-induced disorder are pure colored-noise effects because of the absence in the white-noise limit. We also performed numerical simulations confirming the analytical results.

This work was supported by the Ministry of Information and Communications, Korea. We are grateful to Dr. E. H. Lee for his support of this research.

-
- [1] P. de Kepper and W. Horsthemke, *C. R. Acad. Sci. Ser. C* **187**, 251 (1987).
- [2] J. García-Ojalvo, A. Hernández-Machado, and J. M. Sancho, *Phys. Rev. Lett.* **71**, 1542 (1993).
- [3] A. Becker and L. Kramer, *Phys. Rev. Lett.* **73**, 955 (1994).
- [4] C. Van den Broeck, J. M. R. Parrondo, and R. Toral, *Phys. Rev. Lett.* **73**, 3395 (1994); C. Van den Broeck, J. M. R. Parrondo, J. Armero, and A. Hernández-Machado, *Phys. Rev. E* **49**, 2639 (1994); C. Van den Broeck, J. M. R. Parrondo, and R. Toral, and R. Kawai, *ibid.* **55**, 4084 (1997).
- [5] G. Grinstein, M. A. Muñoz, and Y. Tu, *Phys. Rev. Lett.* **76**, 4376 (1996).
- [6] J. M. R. Parrondo, C. Van den Broeck, J. Buceta, and J. de la Rubia, *Physica A* **224**, 153 (1996).
- [7] S. Kim, S. H. Park, and C. S. Ryu, *Phys. Rev. E* **54**, 6042 (1996); *ETRI J.* **18**, 147 (1996); *Phys. Rev. E* **56**, 3850 (1997).
- [8] J. García-Ojalvo, P. M. R. Parrondo, J. M. Sancho, and C. Van den Broeck, *Phys. Rev. E* **54**, 6918 (1996).
- [9] S. Kim, S. H. Park, and C. S. Ryu, *Phys. Rev. Lett.* **78**, 1616 (1997).
- [10] S. Kim, S. H. Park, and C. S. Ryu, *Phys. Rev. Lett.* **78**, 1827 (1997).
- [11] S. Kim, S. H. Park, and C. S. Ryu, *Phys. Rev. Lett.* **79**, 2911 (1997).
- [12] W. Horsthemke and R. Lefever, *Noise-Induced Transitions* (Springer-Verlag, New York, 1984).